Relativistic and charge-displacement self-channeling of intense ultrashort laser pulses in plasmas

A. B. Borisov*
Laboratory for Computer Simulation, Research Computer Center, Moscow State University, 119 899 Moscow, Russia

A. V. Borovskiy
General Physics Institute, Academy of Sciences of Russia, 117 942 Moscow, Russia

O. B. Shiryaev*
Laboratory for Computer Simulation, Research Computer Center, Moscow State University, 119 899 Moscow, Russia

V. V. Korobkin and A. M. Prokhorov
General Physics Institute, Academy of Sciences of Russia, 117 942 Moscow, Russia

J. C. Solem
Theoretical Division, Los Alamos National Laboratory, Los Alamos, New Mexico 87545

T. S. Luk, K. Boyer, and C. K. Rhodes
Department of Physics, University of Illinois at Chicago, Chicago, Illinois 60680
(Received 25 June 1991; revised manuscript received 20 November 1991)

A simple derivation in the Coulomb gauge of the nonlinear Schrödinger equation describing propagation of powerful ultrashort circularly polarized laser pulses in underdense cold inhomogeneous plasmas is presented. Numerical solutions are given for the two-dimensional axisymmetric case for both initially homogeneous plasmas and static preformed plasma columns. These solutions account for (i) diffraction, (ii) refraction arising from variations in the refractive index due to the spatial profile of the electron density distribution, (iii) the relativistic electronic mass shift, and (iv) the charge displacement resulting from the transverse ponderomotive force. The most important spatial modes of propagation corresponding to (1) purely relativistic focusing and (2) the combined action of both the relativistic and charge-displacement mechanisms are described. The latter leads to the formation of stable confined modes of propagation having paraxially localized regions of high intensity and corresponding paraxially situated cavitated channels in the electron density. It is further demonstrated that the dynamical solutions of the propagation tend asymptotically to the lowest eigenmodes of the governing nonlinear Schrödinger equation. Finally, the calculations illustrate the dynamics of the propagation and show that the relativistic mechanism promotes the initial concentration of the radiative energy and that the subsequent charge displacement stabilizes this confinement and produces waveguidelike channels.

PACS number(s): 52.40.Nk, 42.65.Jx, 52.35.Mw, 52.40.Db

I. INTRODUCTION

The interaction of relativistically intense subpicosecond laser pulses with gaseous media has been an area of vigorous research for the past several years. For ultraviolet wavelengths on the order of 200–300 nm, the intensity region of interest, in which relativistic effects become important, lies above $\sim 10^{18}$ W/cm^2. The propagation of radiation in such media, for intensities greater than $\sim 10^{16}$ W/cm^2, naturally causes strong nonlinear ionization in all matter. Hence, the pulse itself, even in regions where the intensity is relatively low compared to the peak value, removes many electrons [1,2] from the atomic or molecular constituents creating a plasma column in which the main high-intensity component of the pulse propagates. Therefore, in a reasonable first approximation, the investigation of the resulting propagation can be divided into two separate and distinct areas. They are (1) the atomic and plasma physics occurring in the field of the intense electromagnetic wave leading to the ionization and (2) the subsequent nonlinear propagation of the radiation in the plasma that is generated. The work described below concerns the latter issue.

To our knowledge, Akhiezer and Polovin published the first treatment of high-intensity electromagnetic waves in a cold plasma [3]. They derived the equations describing the propagation as a function of the single canonical argument $(\omega t - kz)$ appropriate for one-dimensional wave motion, reduced the problem to Lagrangian form with two integrals of motion, and presented either exact or approximate solutions corresponding to particular simplified special cases.

Several subsequent treatments have been devoted to the acceleration of charged particles in either relativistic beat waves or in the tail of a single relativistic pulse. Specifically, Noble [4] applied the equations derived by Akhiezer and Polovin to the study of single- and double-wave propagation. In other work [5] beat waves in hot

plasmas are described kinetically. The excitation of particles in cold plasmas occurring in the tail of a single intense laser pulse has also been investigated [6].

Importantly, this previous work [6], which considered the case of linear polarization, established that harmonics of the fundamental frequency are not produced at a significant power, if the plasma is underdense and the group velocity of light is close to the speed of light.

Utilizing the quasistatic approximation for the fluid equations of cold underdense plasmas, Sprangle, Esarey, and Ting [7] derived the first nonlinear, fully self-consistent set of equations describing the propagation of relativistic laser pulses into plasmas for a one-dimensional geometry. This formulation was used to obtain insight into relativistic self-focusing, including the self-consistent electron-density profiles, wake-field generation, optical guiding, and second-harmonic generation. However, since this treatment was one-dimensional, the multidimensional case remained unsolved.

An important finding of Sprangle, Esarey, and Ting [7] concerned the diffractional erosion of the leading edge of a pulse propagating in the plasma. However, in the work described below, we concentrate on the evolution of the central portion of the pulse as it propagates in the plasma and neglect the associated erosion of the leading edge.

Extensive literature exists on the motion of electrons in radiation fields of certain explicitly given forms. The solution for the case of plane monochromatic waves is known [8], and this result has been considerably extended in subsequent work [9,10]. Of course, the well-established Volkov solution for the Dirac equation also exists [11]. In particular, Bardsley, Penetrante, and Mittleman [12] have numerically simulated the relativistic dynamics of electrons in a one-electron picture that includes the effects of space charge and the spatial distribution of the radiation field.

The first treatment of the relativistic self-focusing in plasmas was developed by Max, Arons, and Langdon [13]. In addition, the general character of the electromagnetic propagation in plasmas has undergone considerable analysis. Schmidt and Horton [14], Hora [15], and Sprangle *et al.* [16,17] have evaluated the thresholds for relativistic self-focusing using analytic methods. Especially germane is the work of Sun *et al.* [18], who, for initially homogeneous plasmas, derived the two-dimensional (r,z) nonlinear Schrödinger equation governing propagation, including consideration of the combined effect of the relativistic nonlinearity and charge displacement. This work presented the lowest eigenmode of the nonlinear Schrödinger equation and included numerical evaluation of the threshold of relativistic self-focusing, the value of which has been approximately estimated in earlier work [14–17]. Finally, this analysis [18] presented the (r,z) dynamics of the propagation for the perturbed lowest eigenmode of the nonlinear Schrödinger equation for cases not involving spatial cavitation of the electron density. We note that Kurki-Suonio, Morrison, and Tajima [19] have also developed the stationary analytic solutions to this equation for a one-dimensional geometry.

Additional related works can be cited in this context. Relativistic self-focusing and beat-wave phase-velocity control in plasma accelerators are kindred subjects [20]. Computations involving particle simulations revealing the initial process of self-focusing and subsequent ponderomotively driven electron motions have been performed [21]. Other calculations analyzing the plasma dynamics and self-focusing in heat-wave accelerators [22], as well as the consideration of the nonlinear focusing of coupled waves [23], have also appeared.

In prior publications, we have (1) investigated the general behavior of two-dimensional (r,z) axisymmetric relativistic self-focusing, (2) presented results on the process of stabilization of laser pulses in plasma columns [24], (3) described, with the use of an analytical model [25], the steady-state characteristics in cavitated channels having overdense walls, (4) reported preliminary results of calculations that evaluated the combined action of the relativistic and charge-displacement mechanisms and indicated the formation of stable confined cavitated modes of propagation [26], and (5) presented the experimental evidence of relativistic and charge-displacement self-channeling of intense subpicosecond ultraviolet radiation in plasmas [27], including specific comparison with the results of this computational model [27].

The current work presents a full description of the theory of nonlinear propagation of intense axisymmetric ultrashort laser pulses in cold underdense plasmas. In this analysis we use the term ultrashort to indicate that the duration of the pulses τ satisfies the inequality $\tau_i \gg \tau \gg \tau_e$, with τ_i and τ_e designating the response times of the ions and electrons, respectively. We consider both homogeneous plasmas and preformed plasma columns. In this study, no attempt is made to establish consistency between the local ionization state and the local laser intensity, the issue outlined in Sec. I. For sufficiently-low-Z materials, such as hydrogen (H_2), this calculation would be unimportant, since full (maximal) ionization would be achieved even in rather low intensity ($\sim 10^{15}$–10^{16} W/cm^2) regions [28]. Since the main regime of interest for this work involves intensities greater than $\sim 10^{18}$ W/cm^2, we believe that the plasma conditions we have chosen for analysis are sufficiently close to the true self-consistent state to be adequate for the intended scope of this study.

The calculations discussed below have been performed with the specific goal of exploring the characteristic dynamics and stability of the propagation, including particularly, the interplay of the relativistic and charge-displacement processes. Therefore, in order to illustrate this behavior, numerical results are presented that portray the propagation and self-focusing action as a consequence of (1) the purely relativistic nonlinearity and (2) the combined action of the relativistic and charge-displacement mechanisms. Although the relativistic influence cannot be truly physically separated from the charge-displacement process, it has been examined separately because this comparison provides insight on the dynamics of the focusing action, specifically the process by which the charge-displacement and the confined propagation in the electronically cavitated channel develop. Since both the relativistic effect and the charge displace-

ment tend to locally produce a reduction in the plasma frequency (ω_p) that is more significant in the high-intensity regions, both of these effects perturb the wave fronts in a manner that encourages convergence of the wave and the formation of localized high-intensity zones. Furthermore, for both the purely relativistic and the combined cases, we have calculated the stationary eigenmodes of the nonlinear Schrödinger equation and show their relationship to the modes of propagation dynamically developed in the plasmas. In particular, it is shown that the charge displacement, especially that resulting in dynamical cavitation, has a very strong effect on the spatial character of the propagation [26].

The calculations indicate that the efficiency of confinement of the propagating energy is potentially high, namely, that a large fraction of the incident power can be trapped in a channeled mode by the combined action of the relativistic and charge-displacement processes. Furthermore, in the asymptotic regime, it is found that the channel is characterized spatially by an intensity profile and electron-density distribution corresponding to the lowest z-independent eigenstate of the nonlinear Schrödinger equation. Overall, the principal conclusion of this work is that, under appropriate conditions, a new dynamical mode of *stable highly confined propagation* naturally evolves for the propagation of sufficiently short ($\tau_i \gg \tau \gg \tau_e$) pulses of coherent radiation in plasmas. By new dynamical modes, we mean the self-channeling of the radiation through the formation of stabilized electronically cavitated paraxial modes, which result from the combined action of the relativistic and charge-displacement mechanisms. Interestingly, for ultraviolet wavelengths in the (200–300)-nm range, the power densities naturally associated with these environments can approach thermonuclear values.

In Sec. II the underlying physical concepts are presented and the governing nonlinear Schrödinger equation is derived. Section III presents the analysis of the eigenmodes of this equation. Representative results of numerical simulations of the two-dimensional axisymmetric propagation are given in Sec. IV. Section IV also contains a comparison with the purely relativistic case. Finally, the conclusions are summarized in Sec. V.

II. GENERAL CONSIDERATIONS

A. Physical model

Several physical phenomena [1–7,14–19,24–26,29] play a role in the nonlinear dynamics governing the propagation of intense coherent radiation under the conditions being examined in this study. They are the following.

(a) The creation of a plasma column by ionization in the temporally early region of the laser pulse.

(b) The influence of the spatial variation of the refractive index arising from the nonlinear response of the dielectric properties of the medium. Two mechanisms are related to the electronic component; specifically, the relativistic shift in electron mass and the ponderomotively driven electron motion which tends to displace electrons from the high-intensity zone. For sufficiently short pulses, only the electrons are expelled from the laser beam and the more massive ions, due to their substantially greater inertia, are regarded as motionless [17,18,25]. A third mechanism is the nonlinear response arising from the induced dipoles of the ions, but this is generally small and negligible [25].

(c) Defocusing mechanisms, caused by diffraction from the finite aperture and refraction by the transverse inhomogeneities in the electron density.

(d) Dissipation of laser-beam energy by (i) motion of the electrons, (ii) ionization of the gas atoms, (iii) generation of harmonic radiation, (iv) production of inverse bremsstrahlung, (v) Compton scattering, and (vi) other amplitudes of nonlinear scattering.

The present work incorporates four phenomena: (1) the nonlinear response of the refractive index of the plasma due to the relativistic increase in the mass of the free electrons, (2) the refractive index variation due to the perturbation of the electron density by the ponderomotive force, (3) the diffraction caused by the finite aperture of the propagating energy, and (4) the refraction generated by the transversely inhomogeneous plasma density associated with the formation of a plasma column. In these calculations, preformed static plasma columns were used in order to approximate the radial distribution of ionization that is expected, if the incident laser pulses were producing the ionization on their temporally leading edge. Finally, the calculations were performed for a length of propagation that is much shorter than the characteristic length for dissipation of the energy of the pulse through ionization or other modes of energy loss.

It should be noted that the relativistic intensities characteristic of the phenomena examined in this work can be currently obtained experimentally [30–32]. In particular, the experimental parameters characteristic of the ranges that would apply to the study of these phenomena are presented in Table I. With the wavelength and range of electron densities shown in Table I, the plasma is always underdense, namely, $(\omega_p/\omega)^2 \ll 1$, where $\omega = 2\pi c/\lambda$ is the angular frequency of the laser radiation and $\omega_p = (4\pi e^2 N_e/m_e)^{1/2}$ is the customary plasma frequency.

B. The propagation equation

Consider the propagation of an intense ultrashort laser pulse in a plasma with an initially radially inhomogeneous electron density, described by the function $f(r)$, so

TABLE I. Experimental parameters characteristic of the ranges that would apply for the study of relativistic and charge-displacement self-focusing of laser pulses in plasmas.

Peak intensity	$I \simeq 10^{18}$–10^{20} W/cm^2
Pulse length	$\tau \simeq 100$–1000 fs
Initial focal spot radius	$r_0 \simeq 1$–3 μm
Wavelength	$\lambda \simeq 0.248$ μm (KrF* laser light)
Target gas densities	$\rho \simeq 10^{16}$–10^{20} cm^{-3}
Initial unperturbed electron density	$N_e \simeq 10^{17}$–10^{21} cm^{-3}

that $N_e^{(0)}=N_{e,0}f(r)$, $\max f(r)=1$. We denote the vector and the scalar potentials of the electromagnetic fields as $\mathbf{A}$ and ϕ, respectively, and the corresponding electric field as $\mathbf{E}$. Let the momentum of the electrons, the current density, and the charge density be denoted as $\mathbf{P}_e$, $\mathbf{j}$, and ρ, respectively. We assume, for the short timescale of interest, that the ions are inertially frozen in space [17,18,24,25]. Then,

$$\Box\mathbf{A}=c^{-1}\nabla\frac{\partial\phi}{\partial t}-(4\pi/c)\mathbf{j}\ , \tag{1}$$

$$\nabla^2\phi=-4\pi\rho\ , \tag{2}$$

$$(\nabla\cdot\mathbf{A})=0\ , \tag{3}$$

$$\left[\frac{\partial}{\partial t}+(\mathbf{v}_e\cdot\nabla)\right]\mathbf{p}_e=-e\left[-c^{-1}\frac{\partial\mathbf{A}}{\partial t}-\nabla\phi+c^{-1}[\mathbf{v}_e\times(\nabla\times\mathbf{A})]\right]\ , \tag{4}$$

$$\mathbf{j}=-eN_e\mathbf{v}_e,\quad \rho=e(N_e^{(0)}-N_e)\ , \tag{5}$$

$$\mathbf{v}_e=\mathbf{p}_e/m_e,\quad m_e=m_{e,0}\gamma\ ,\quad \gamma=[1+|\mathbf{p}_e|^2/(m_{e,0}c)^2]^{1/2}\ . \tag{6}$$

In the set of statements above, Eqs. (1) and (2), are the Maxwell equations, Eq. (3) is the Coulomb gauge condition, Eq. (4) is the equation of motion of the electrons, Eqs. (5) are the definition of the current density and the charge density ($N_e^{(0)}$ is the initial charge density, while N_e is the dynamical charge density), and Eqs. (6) represent the relativistic relation between the velocity $\mathbf{v}_e$ and the momentum of the electrons. In Eqs. (6), $m_{e,0}$ is the rest electron mass, $\Box=\nabla^2-c^{-2}\partial^2/\partial t^2$.

It is convenient to normalize the values in the equations presented above as follows:

$$\tilde{\mathbf{A}}=(e/m_{e,0}c^2)\mathbf{A},\quad \tilde{\phi}=(e/m_{e,0}c^2)\phi\ ,\quad \tilde{\mathbf{E}}=(e/m_{e,0}c^2)\mathbf{E}\ ,\quad \tilde{\mathbf{p}}_e=\mathbf{p}_e/m_{e,0}c\ ,\quad \tilde{\mathbf{v}}_e=\mathbf{v}_e/c,\quad \tilde{N}_e=N_e/N_{e,0}\ , \tag{7}$$

with the understanding that, henceforth, the tilde sign will be suppressed. Using the relations $(\mathbf{p}_e\cdot\nabla)\mathbf{p}_e=\nabla|\mathbf{p}_e|^2/2-\mathbf{p}_e\times(\nabla\times\mathbf{p}_e)$ and $\nabla\gamma=\nabla|\mathbf{p}_e|^2/2\gamma$, Eq. (4) becomes

$$\frac{\partial}{\partial t}(\mathbf{p}_e-\mathbf{A})-\mathbf{v}_e\times[\nabla\times(\mathbf{p}_e-\mathbf{A})]=\nabla(\phi-\gamma)\ . \tag{8}$$

In the limit $\tau\gg 2\pi/\omega_\rho$, the expression $\mathbf{p}_e=\mathbf{A}$ is approximately valid. As we shall see below, this condition means that the electron response can be regarded as adiabatic. Furthermore, assuming the vector potential to be circularly polarized, we write

$$\mathbf{A}(r,z,t)=\tfrac{1}{2}\{(\mathbf{e}_x+i\mathbf{e}_y)a(r,z,t)\exp[i(\omega t-kz)]+\text{c.c.}\}\ . \tag{9}$$

Consistent with the statements made above, we emphasize the use of the assumption that the pulse length in both space and time is much greater than both the plasma ($2\pi c/\omega_{\rho,0}$) and electromagnetic (λ) wavelengths. This leads to the validity of the inequalities

$$\left|c^{-1}\frac{\partial a}{\partial t}\right|,\ \left|\frac{\partial a}{\partial z}\right|\ll|ka|,|k_pa|\ ,$$

where $k^2=k_0^2-k_p^2$, $k_0=\omega/c$, and $k_p=\omega_{p,0}/c$. We use the notation $\omega_{p,0}^2=4\pi e^2N_{e,0}/m_{e,0}$ specifically to denote the unperturbed plasma frequency. With the assumptions and approximations stated above, Eqs. (1)–(8) become

$$\Box\mathbf{A}=k_p^2N_e\gamma^{-1}\mathbf{A}\ , \tag{10}$$

$$\nabla^2\phi=k_p^2[N_e-f(r)]\ , \tag{11}$$

$$\nabla(\phi-\gamma)=0\ , \tag{12}$$

$$\gamma=(1+|\mathbf{p}_e|^2)^{1/2},\quad \mathbf{p}_e=\mathbf{A}\ . \tag{13}$$

The term $c^{-1}\partial\nabla\phi/\partial t$ is omitted in Eq. (10), since γ and ϕ, according to Eqs. (9), (12), and (13), do not have a high-frequency dependence. Equations (11) and (12) result in the expression for the electron density,

$$N_e=\max[0,f(r)+k_p^{-2}\nabla^2\gamma]\ . \tag{14}$$

The logical function max(0,) provides for the physically obvious and necessary condition $N_e\geq 0$. The analogous expression for the electron density has been previously derived by Sun *et al.* [18] for the case $f(r)\equiv 1$. It should be noted that Eq. (12) states the condition for the balance of the ponderomotive and the electrostatic forces for the relativistic case. Through combining Eqs. (9), (10), and (14), we establish the equation for the slowly varying complex amplitude of the vector potential $a(r,z,t)$ as

$$\left[\frac{1}{v_g}\frac{\partial}{\partial t}+\frac{\partial}{\partial z}\right]a+\frac{i}{2k}(\nabla_\perp^2a+k_p^2\{1-\gamma^{-1}\max[0,f(r)+k_p^{-2}\nabla_\perp^2\gamma]\}a)=0\ . \tag{15}$$

In accord with the previous assumptions used in deriving Eq. (15), we have neglected the second z and t derivatives in this expression. In Eq. (15), $v_g=c\epsilon_0^{1/2}$ is the group velocity of light in unperturbed plasma, $\epsilon_0=1-(\omega_{p,0}/\omega)^2$ is its corresponding dielectric constant, and $\gamma=(1+|a|^2)^{1/2}$. It should also be noted that the electric field vector $\mathbf{E}$ and the vector potential $\mathbf{A}$ are related through the approximate relation

$$\mathbf{E}(r,z,t)\simeq -ik_0\mathbf{A}(r,z,t)\ .$$

The calculation of the propagating wave form for the central high-intensity region of the pulse is accomplished by considering the solutions of Eqs. (15) along its characteristics. Changing the variable t to $q\equiv t-z/v_g$, Eq. (15) becomes

$$\frac{\partial}{\partial z}a+\frac{i}{2k}(\nabla_\perp^2 a+k_p^2\{1-\gamma^{-1}\max[0,f(r)+k_p^{-2}\nabla_\perp^2\gamma]\}a)=0\ , \quad (16)$$

for which we seek solutions of the form $q\equiv$const. We recall that certain solutions of Eq. (16) for the special case $f(r)\equiv 1$ have already been presented [18,19,33].

The results of the computations presented in this work are given with respect to the variables (q,r,z). Specifically, the data presented in the figures below illustrate the propagation of the radiation along the z axis for $q\equiv$const. Equation (16) describes the two-dimensional (r,z) dynamics of propagation for coherent circularly polarized radiation in plasmas having an inhomogeneous transverse (r-dependent) distribution of electron density. The basic physical phenomena explicitly embodied in these equations have been outlined in Sec. II A.

III. STATIONARY SELF-LOCALIZED MODES OF PROPAGATION

Equation (16), in the case of homogeneous plasmas $[f(r)\equiv 1]$, has axisymmetric partial solutions of the form

$$a(r,z)=U_{s,n}(k_p r)\exp[i(k_p^2/2k)(s-1)z]\ , \quad (17)$$

where s is a real-valued dimensionless parameter and the real-valued function $U_{s,n}$ obeys the ordinary differential equation [18]

$$\nabla_\perp^2 U_{s,n}+[s+F(U_{s,n}^2)]U_{s,n}=0\ . \quad (18)$$

In this discussion the dimensionless argument $\rho=k_p r$ is used and $\nabla_\perp^2$ in Eq. (18) denotes the Laplacian with the derivatives designated with respect to this variable (ρ).

The nonlinear term in Eq. (18) is

$$F(U_{s,n}^2)=-N_{s,n}/\gamma_{s,n}\ ,$$
$$N_{s,n}=\max(0,1+\nabla_\perp^2\gamma_{s,n})\ , \quad (19)$$
$$\gamma_{s,n}=(1+U_{s,n}^2)^{1/2}\ .$$

The natural boundary conditions for Eq. (18) are

$$\frac{dU_{s,n}(0)}{d\rho}=0,\quad U_{s,n}(\infty)=0\ . \quad (20)$$

The first condition assures axial symmetry of the solutions, while the second is necessary for the property of finite energy for the solutions. We designate these solutions as "eigenmodes" and their significance is explored below.

Consider initially, however, the eigenmodes corresponding to the purely relativistic case, functions which are obtained from Eqs. (18) and (19) by neglecting the term $\nabla_\perp^2\gamma_{s,n}$. Since, we are explicitly eliminating the ponderomotive potential and its influence on the motion of the electrons, in this situation the electron density will not be self-consistent. In this restricted case, Eq. (18) can be rewritten in the form

$$\frac{d}{d\rho}\left[\tfrac{1}{2}\left[\frac{dU_{s,n}}{d\rho}\right]^2+V(U_{s,n},s)\right]=-\rho^{-1}\left[\frac{dU_{s,n}}{d\rho}\right]^2\ ,$$

where $V(U_{s,n},s)=(s/2)U_{s,n}^2-(1+U_{s,n}^2)^{1/2}+1$.

The second boundary condition, stated in Eq. (20), ensures finiteness of energy only in the situation where the dynamical system defined by the last two expressions has three rest points, one of them being zero, that is for the case $0<s<1$. Exactly as in the classic theory of cubic media [34,35] for values of the parameter s belonging to this interval, the localized eigenmodes constitute a countable set that is ordered by the number of zeros–n in each of its members for finite values of ρ. Figure 1 illustrates the first four eigenmodes for $s=0.95$.

Consider now the eigenmode corresponding to the unrestricted situation that includes both the relativistic and charge-displacement mechanisms, a case which is found to be fully analogous. The eigenmodes of the equation describing the combined relativistic and charge-displacement processes for the interval $0<s<1$ *also* make a countable set that can be ordered in the same way as the one associated with the purely relativistic case. The zeroth (lowest) eigenmode $U_{s,0}(\rho)$ with $s=0.95$, along with the corresponding electron density $N_{s,0}(\rho)$, given by the second formula in Eq. (19), are depicted in Fig. 2. These two functions have been developed in earlier work [18]. The first and second relativistic and charge-displacement eigenmodes for the value of the parameter $s=0.95$ and the corresponding electron-density eigenmodes $N_{s,1}(\rho)$ and $N_{s,2}(\rho)$ are depicted in Figs. 3 and 4, respectively. These higher eigenmodes exhibit the important feature that cavitation may occur in the electronic component of plasma [see Fig. (4)], *even if it does not occur* in the case of the lower eigenmodes [see Figs. 2 and 3].

A prior study [18] treated the (r,z) dynamics of the evolution of the perturbed lowest eigenmodes for the case in which no cavitation of the electronic component of plasma occurs. The lowest eigenmodes were perturbed by multiplying them by constants in the neighborhood of unity. In this case, the known regime involving oscillatory propagation was observed. However, the instability of the numerical method applied in that work [18] prevented the performance of similar computations for cases involving cavitation. Our calculations show that the analogously perturbed lowest eigenmodes $V_{s,0}(\rho)$ also propagate in the same oscillatory fashion when electronic cavitation occurs, the corresponding density of which is given by $N_{s,0}(\rho)$. It is also found that the same behavior devel-

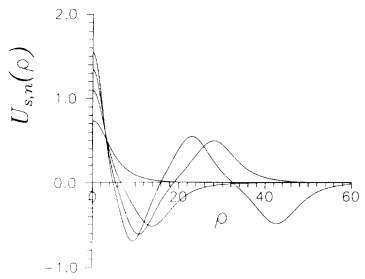

FIG. 1. Stationary axially symmetric eigenmodes with $s=0.95$ corresponding to purely relativistic self-focusing.

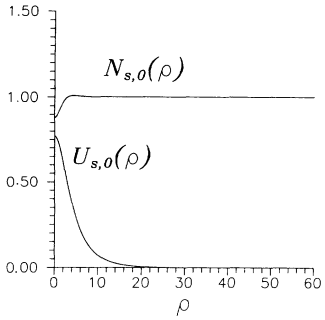

FIG. 2. The zeroth (lowest) axially symmetric stationary eigenmode with $s=0.95$ corresponding to relativistic and charge-displacement self-focusing: the normalized field amplitude distribution $U_{s,0}(\rho)$ and the normalized electron density distribution $N_{s,0}(\rho)$.

ops for the perturbed first eigenmodes, which have one or two cavitated channels in the electronic density described by $N_{s,1}(\rho)$. The results of these simulations can be regarded as evidence of the (r,z) stability of axially symmetric lowest and first eigenmodes against small perturbations in the amplitude. It should be noted, however, that these higher eigenmodes are presumably unstable against small *azimuthal* perturbations, the nature of which violates the assumed axial symmetry of the distributions.

The important consequence of the character of the solutions discussed above is the fact that the power

$$P_s=2\pi\int_0^\infty U_{s,0}^2(\rho)\rho\,d\rho$$

contained in the intensity distribution corresponding to the lowest eigenmode $U_{s,0}(\rho)$, unlike the case of a cubic medium, depends on the parameter s. Namely, this power decreases as s increases.

The infimum of P_s by s, in the internal $0<s<1$, is called the critical power ($P_{\rm cr}$) of the relativistic and charge-displacement self-focusing. This power equals the critical power of the purely relativistic self-focusing [18,36] and

$$P_{\rm cr}=\inf_{0<s<1}P_s=\lim_{s\to 1-0}P_s\ .$$

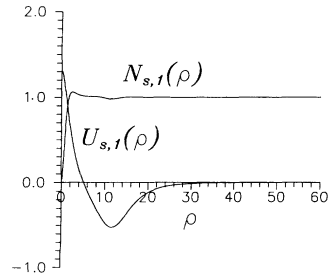

FIG. 3. The first axially symmetric stationary eigenmode with $s=0.95$ corresponding to relativistic and charge-displacement propagation: the normalized amplitude distribution $U_{s,1}(\rho)$ and the normalized electron-density distribution $N_{s,1}(\rho)$.

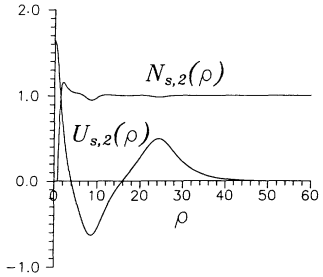

FIG. 4. The second axially symmetric stationary eigenmode with $s=0.95$ corresponding to relativistic and charge-displacement propagation: the normalized amplitude distribution $U_{s,2}(\rho)$ and the normalized electron-density distribution $N_{s,2}(\rho)$.

The explicit evaluation of this critical value is presented below. As $U_{s,0}(\rho)\to 0$, $N_{s,0}(\rho)\to 1$ for $s\to 1-0$; we have [18] therefore,

$$\gamma_{s,0}^{-1}N_{s,0}-1=N_{s,0}(1+U_{s,0}^2)^{-1/2}-1 \underset{s\to 1-0}{\approx}(1+U_{s,0}^2/2)^{-1}-1\underset{s\to 1-0}{\approx}-U_{s,0}^2/2\ .$$

Furthermore,

$$U_{s,0}(\rho)\underset{s\to 1-0}{\approx}U_0(\rho)\ ,$$

where $U_0(\rho)$ is the positive, monotonically decreasing (reaching zero for no finite value of ρ) solution to the boundary-value problem [18,36]

$$\nabla_\perp^2U_0-\epsilon U_0+\tfrac{1}{2}U_0^3=0\ ,$$

$$\frac{dU_0}{d\rho}(0)=0,\quad U_0(\infty)=0\ ,$$

with $\epsilon=1-s$. A change of the variables, which is a standard procedure for treating the case of the cubic nonlinearity [37], shows that [36]

$$U_0(\rho)=(2\epsilon)^{1/2}g_0(\epsilon^{1/2}\rho)\ ,$$

where g_0 is the customary Townes mode, i.e., the positive, monotonically vanishing solution to the following boundary-value problem:

$$\nabla_\perp^2g_0-g_0+g_0^3=0\ ,$$

$$\frac{dg_0}{d\rho}(0)=0,\quad g_0(\infty)=0\ .$$

From the definition of $P_{\rm cr}$ and the relation between $U_0(\rho)$ and $g_0(\rho)$, it follows that

$$P_{\rm cr}=\inf_{0<s<1}P_s=\lim_{s\to 1-0}P_s=2\pi\int_0^\infty U_0^2(\rho)\rho\,d\rho=4\pi\int_0^\infty g_0^2(\rho)\rho\,d\rho=2P_{{\rm cr},c}\ ,$$

where $P_{{\rm cr},c}\equiv 2\pi\int_0^\infty g_0^2(\rho)\rho\,d\rho$ is the critical power of the Kerr self-focusing in cubic media [34,37].

Using the resulting relation between the normalized values of the critical power of the relativistic and charge-

displacement self-focusing P_{cr} and the critical power of the Kerr self-focusing $P_{cr,c}$ we have the elementary result that

$$P_{cr}=2P_{cr,c} .$$

Finally, by calculating $g_0(\rho)$ numerically, we find the normalized value of P_{cr} with high precision [36] to be

$$P_{cr}=2P_{cr,c}=4\pi\int_0^\infty g_0^2(\rho)\rho\, d\rho\simeq 23.4018 .$$

Hence, we establish the expression for the critical power [36] as

$$P_{cr,1}=(m_{e,0}^2c^5/e^2)\int_0^\infty g_0^2(\rho)\rho\, d\rho(\omega/\omega_{p,0})^2 \simeq 1.6198\times 10^{10}(\omega/\omega_{p,0})^2 \text{ W} .$$

The constant factor involved in this statement improves on that given previously [18].

The relation between $U_0(\rho)$ and $g_0(\rho)$ enables the development of the asymptotic expressions (in the case $\epsilon\to 0$) for both the peak value of the amplitude of the stationary eigenmode and for the radius of the eigenmode by using the appropriate characteristics of the Townes mode. The results are

$$U_{s,0}(0)\simeq(2\epsilon)^{1/2}g_0(0)$$

and

$$r_s\simeq\epsilon^{-1/2}r_0 ,$$

for $\epsilon\to 0$.

Special computations were performed in order to determine how close the values for $U_{s,0}(0)$ and $U_0(0)=(2\epsilon)^{1/2}g_0(0)$ are in the case where $\epsilon\ll 1$. The calculations show that $|U_{s,0}(0)-U_0(0)|/U_0(0)$ is 2.026×10^{-5} and 2.096×10^{-6} for $\epsilon=10^{-5}$ and 10^{-6}, respectively.

IV. THE TWO-DIMENSIONAL CASE

It is convenient to treat Eq. (16) numerically using the normalized coordinates

$$r_1=r/r_0 , \quad z_1=z/(2kr_0^2) ,$$

$$u(r_1,z_1)=a_0^{-1}a(r,z) ,$$

where r_0 is a characteristic radius of the initial intensity profile and $a_0=\max|a(r,0)|$ for the selected value of q. For simplicity, we put $f_1(r_1)=f(r)$ and omit below the subscript 1 of r_1 and z_1 for brevity. Thus, the mathematical statements can be expressed in the following set of equations:

$$\frac{\partial u}{\partial z}+i\nabla_\perp^2u+iF(f_1(r),|u|^2)u=0, \quad z>0 \tag{21}$$

$$u(r,0)=u_0(r), \quad \max_r|u_0|=1 \tag{22}$$

$$\frac{\partial u}{\partial r}(0,z)=0, \quad u(\infty,z)=0 . \tag{23}$$

The nonlinear term F is the real-valued operator

$$F(f_1,\xi)=a_1\{1-(1+a_2\xi)^{-1/2} \times\max[0,f_1(r)+a_1^{-1}\nabla_\perp^2(1+a_2\xi)^{1/2}]\} , \tag{24}$$

and the dimensionless parameters a_1, a_2 are defined as

$$a_1\equiv(r_0k_p)^2, \quad a_2\equiv I_0/I_r, \quad I_0\equiv m_{e,0}^2\omega^2c^3a_0^2/(4\pi e^2) , \tag{25}$$

where I_0 is the peak intensity at the entrance plane ($z=0$) of the medium. The parameter $I_r=m_{e,0}^2\omega^2c^3/(4\pi e^2)$ is known as the relativistic intensity [15].

The ratio of the power of the beam P_0 and the critical power of the relativistic and charge-displacement self-focusing P_{cr}, defined in Sec. III, is an important parameter characterizing Eqs. (21)–(24). In the notations of the present section, the value of P_0/P_{cr} can be expressed in the following way [36]:

$$P_0/P_{cr}=(a_1a_2/B)\int_0^\infty|u_0(r)|^2r\, dr ,$$

with dimensionless constant B given by [36]

$$B=2\int_0^\infty g_0^2(\rho)\rho\, d\rho\simeq 3.724\,51 .$$

When the initial transverse-intensity distribution is Gaussian, namely, $|u_0(r)|^2=\exp(-r^2)$, we have

$$P_0/P_{cr}=a_1a_2/(2B) .$$

We note that in several other studies, the critical power of the relativistic self-focusing is defined alternatively, basically with $B=4.0$. In the present discussion, the expression for P_0/P_{cr} involves a value of $B<4.0$, so that the corresponding ratio P_0/P_{cr} is raised. Therefore, a pulse having a Gaussian initial transverse-intensity distribution and a flat initial wave front with the parameters $a_1=248.6192$ and $a_2=0.031$, undergoes self-focusing. In this case, the ratio P_0/P_{cr}, as defined above, evaluates to 1.0347, namely, $P_0>P_{cr}$. However, using the value $B=4.0$ would give $P_0<P_{cr}$, a statement contradicting the results of the computations.

A. The initial conditions

In this section, we examine the self-focusing of coherent radiation for pulses having Gaussian or hyper-Gaussian transverse and longitudinal intensity distributions [24] of the form

$$I|_{z=0}=I_0(r,t)=I_m\exp[-(t/\tau)^{N_1}-(r/r_0)^{N_2}] , \quad N_1\geq 2, \quad N_2\geq 2 \tag{26}$$

with r and t being dimensional. We assume [24] that $I_m\simeq I_r\gg I^*=10^{16}\text{ W cm}^{-2}$ with I^* designating the approximate value of the threshold for rapid nonlinear ionization [1,2]. The spatial amplitude distribution of the incident radiation, defined by Eq. (26) for the case of a flat incident phase front, is of the form

$$u_0(r)=\exp(-r^{N_2}/2)\ ,\quad N_2\geq 2\ . \tag{27}$$

The dimensionless parameter a_2 in Eq. (25), corresponding to the incident pulse intensity on the axis ($r=0$) of the beam $I_0(t)$, is

$$a_2=I_0(t)/I_r=(I_m/I_r)\exp[-(t/\tau)^{N_1}]\ . \tag{28}$$

The transverse profile of the plasma column, created by the temporally leading edge of the pulse, is simulated by the hyper-Gaussian function

$$f(r)=\exp[-(r/r_*)^{N_3}],\quad N_3\geq 2\ , \tag{29}$$

where r is the radial coordinate. The aperture of the plasma column r_* can be estimated [24] with the use of the relation

$$I_0(r_*,t_0)\equiv I_0(t_0)\exp[-(r_*/r_0)^{N_2}]=I^*\ . \tag{30}$$

For example, in the case of the Gaussian transverse intensity distribution ($N_2=2$), the aperture of the plasma column for $I^*=10^{16}$ W cm^{-2}, $I_r\simeq 0.45\times 10^{20}$ W cm^{-2}, and $I_0(t_0)=(0.1)I_r$, gives $r_*\simeq 2.47r_0$. In this situation, the homogeneous plasma approximation $f(r)\equiv 1$ is valid [24]. In contrast, it follows from Eq. (30) for plateaulike incident-transverse-intensity distributions that the aperture r_* of the simulated plasma column tends to the value of the beam aperture r_0. Therefore, in the example given above for $N_2=8$, we have $r_*\simeq 1.25r_0$. Thus, defocusing of the beam, which is significant because of the near coincidence of the apertures of the laser beam and the plasma column, must be taken into account when the evolution of a beam with a plateaulike incident-transverse-intensity distribution is studied [24].

B. Relativistic self-focusing

Consider the two-dimensional (r,z) solutions of the system of equations embodied in Eqs. (21), (22), and (23) for the purely relativistic nonlinear term, the form of which can be obtained from Eq. (24) by disregarding the term involving $\nabla_\perp^2$. In this case, we find

$$F(f_1,\xi)=a_1[1-f_1(r)(1+a_2\xi)^{-1/2}]\ .$$

The relativistic self-focusing mechanism prevails over the charge-displacement mechanism outside of the focal spot under the conditions $a_1\gg 1$, $a_2\simeq 1$. (Discussion of the conditions for the prevailing of the relativistic self-focusing can also be found in Ref. [33]). The situation represented by Eqs. (21), (22), and (23), with the above nonlinear term, describes self-focusing with a nondissipative saturation of the nonlinearity. The properties of the solutions for this case depend essentially on the values of two conserved integrals given specifically by

$$P_1=\int_0^\infty |u(r)|^2 r\,dr \tag{31}$$

and

$$P_2=\int_0^\infty \left[\left|\frac{\partial u}{\partial r}\right|^2-\phi(r,|u|^2)\right] r\,dr\ , \tag{32}$$

where

$$\phi(r,\xi)=\int_0^\xi F(r,\eta)d\eta$$
$$=a_1\{\xi-(2/a_2)f_1(r)[(1+a_2\xi)^{1/2}-1]\}\ . \tag{33}$$

Figure 5 illustrates the nature of the calculated solutions corresponding to this purely relativistic case. The parameters of the incident radiation and plasma, for the examples presented in Fig. 5, are $\lambda=0.248$ μm, $I_r=0.45\times 10^{20}$ W cm^{-2}, $I_0=\frac{2}{3}I_r=3\times 10^{19}$ W cm^{-2}, $r_0=3$ μm, and $N_{e,0}=7.5\times 10^{20}$ cm^{-3}. The corresponding values of the associated dimensionless parameters are $a_1\simeq 2.486\,192\times 10^2$ and $a_2=\frac{2}{3}$.

Figure 5(a) presents the result for purely relativistic propagation in a homogeneous plasma along the z axis for a pulse having an incident Gaussian transverse intensity distribution and a flat wave front [$N_2=2$ in Eq. (27)] for the value of q defined in Sec. II B, corresponding to $I_0=\frac{2}{3}I_r$. Figure 5(b) presents the analogous graph for a plateau like incident transverse intensity distribution [$N_2=8$ in Eq. (27)]. We conclude from these results that the solution is critically dependent upon the initial condition represented by the detailed character of the incident transverse intensity distribution.

The ratio of the beam power (P_0) to the critical power (P_{cr}) of the relativistic self-focusing for the given values of the parameters a_1 and a_2 yields $P_0/P_{cr}=22.252$ in the case of the Gaussian initial transverse intensity distribution [$N_2=2$ in Eq. (27), Fig. 5(a)] and $P_0/P_{cr}=20.168$ in the latter example of the plateaulike [$N_2=8$ in Eq. (27), Fig. 5(b)] initial transverse intensity distribution.

Note that for the values of the parameters a_1,a_2 and incident wave forms studied, we have from Eq. (32) $P_2<0$. In this situation, the following inequality is valid:

$$\max_r |u(r,z)|^2>(4/a_1a_2)|P_2|/P_1\ , \tag{34}$$

namely, with respect to the radial coordinate r, the maximum beam intensity has a positive lower bound *independent* of z. This conclusion can be established in the same way that Zakharov, Sobolev, and Synakh [37] demonstrated the analogous result in their earlier work on self-focusing. Therefore, a powerful relativistic beam, which self-focuses in a homogeneous nonabsorbing plasma ($\mu=0$, Ref. [24]), results in a field distribution representing a pulsing waveguide when $P_2<0$. Figures 5(a) and 5(b) explicitly illustrate the formation of such a regime. These pulsing waveguides consist of alternations of ring structures and focal spots on the axis of the beam. The power confined in these complex modes represents approximately 50% and 90% of the total incident power for the cases depicted in Figs. 5(a) and 5(b), respectively. It should be noted that oscillating periodic solutions of this type have also been presented by other workers [17].

In the case $P_2\geq 0$, an inequality comparable to Eq. (34) cannot be obtained. Following the method of Zakharov, Sobolev, and Synakh [37], we simulate the case $P_2\geq 0$ by considering a beam initially focused or defocused by a lens at the entrance plane ($z=0$) of the medium. Let the focusing (or defocusing) length of this lens be $R=kr_0^2R_f$

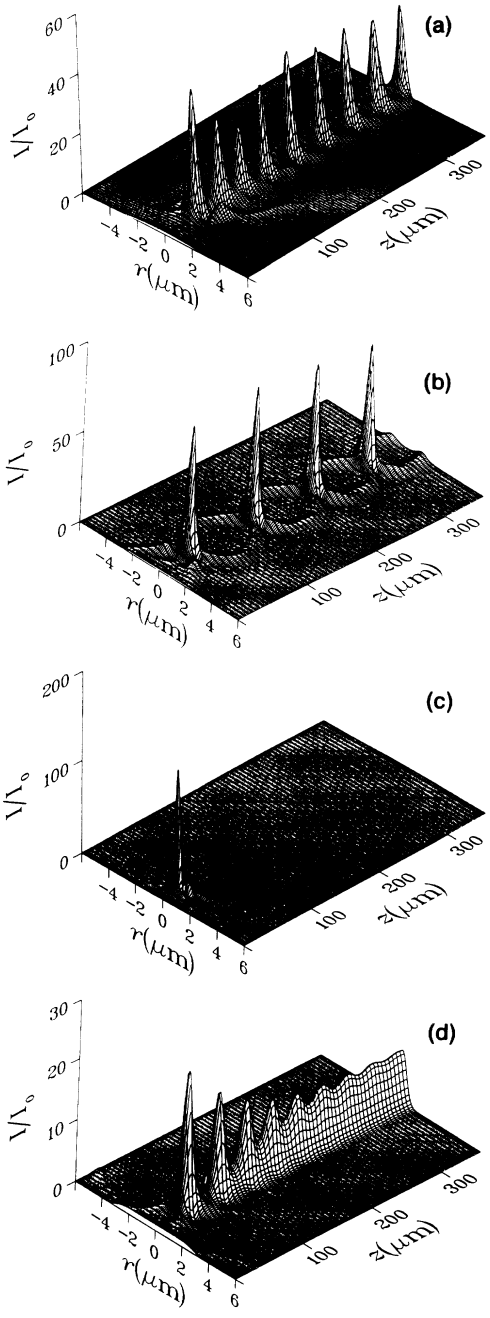

FIG. 5. Purely relativistic propagation with $I_0=3\times10^{19}$ W/cm^2, $r_0=3$ μm, $\lambda=0.248$ μm, and $N_{e,0}=7.5\times10^{20}$ cm^{-3}. (a) The formation of the pulsing waveguide regime in the case of the relativistic self-focusing of a pulse with a flat incident wave front; Gaussian initial transverse-intensity distribution [$N_2=2$ in Eq. (27)], homogeneous plasma. (b) The formation of the pulsing waveguide regime in the case of the relativistic self-focusing of a pulse with a flat incident wave front; hyper-Gaussian initial transverse-intensity distribution [$N_2=8$ in Eq. (27)], homogeneous plasma. (c) The single-focus regime in the case of the relativistic self-focusing of an initially focused pulse [$R_f=R_{f,0}/2$ in Eq. (35)]; Gaussian incident-transverse-intensity distribution [$N_2=2$ in Eq. (35)], homogeneous plasma. (d) The formation of the quasistabilized regime in the case of the relativistic self-focusing of a pulse with a flat incident wave front in a plasma column [$N_3=8$, $r_*=r_0$ in Eq. (29)]; hyper-Gaussian initial transverse-intense distribution [$N_2=8$ in Eq. (27)].

(R_f dimensionless). The condition $R_f>0$ signifies that the pulse is initially focused and $R_f<0$ indicates that it is initially defocused. Then, the corresponding initial condition can be written as

$$u_0(r)=\exp[-r^{N_2}/2+ir^2/(2R_f)], \quad N_2\geq 2 . \tag{35}$$

Furthermore, let $P_2=0$ for $|R_f|=R_{f,0}$. We note that the case $P_2>0$ corresponds physically to a high degree of the initial focusing or defocusing: $R_{f,0}>|R_f|>0$. Moreover, when $R_{f,0}<|R_f|\leq\infty$, $P_2<0$.

Figures 5(a) and 5(c) display the calculated intensity distributions for the case of relativistic self-focusing in homogeneous plasma of beams with Gaussian incident-transverse-intensity distributions and values of R_f given by $R_f=\infty$ (flat wave front) and $R_{f,0}/2$, respectively. A more detailed study of the dynamics of the transition from the pulsing waveguide regime [see Fig. 5(a)], to the single-focus regime [see Fig. 5(c) representing the propagation of an initially sufficiently sharply focused beam)] can be found in Ref. [38]. Importantly, the computations show that the value $P_2=0$ is *not* the threshold separating these two regimes of relativistic self-focusing. This transition occurs as the first focus gains power and is shifted closer to the entrance of the medium ($z=0$), while the remaining foci are shifted in the opposite direction and, in the limit of large displacement, become diffused. Note that single-focus regimes of propagation have also been observed by Sprangle, Tang, and Esarey [17].

Defocused beams can evolve in a different fashion. Initially sufficiently sharply defocused pulses ($R_f<0$, $|R_f|\lesssim R_{f,0}/2$, $P_2>0$) propagating in the relativistic regime monotonically diffuse on the radial periphery and do not exhibit the phenomenon of self-focusing.

The detailed spatial character of the plasma column can have a strong influence on the evolution of the propagation. Figure 5(d) illustrates the relativistic propagation in a plasma column along the z axis for a pulse corresponding to $N_2=8$ in Eq. (27). The transverse profile of the plasma column is given by $f(r)$ as defined by Eq. (29) with $N_3=8$ and $r_*=r_0$. The comparison between Figs. 5(b) and 5(d) demonstrates that the defocusing of a hyper-Gaussian beam in a plasma column, with an aperture close to the radius of the beam, fundamentally alters the spatial dynamics of the propagating energy [24]. The defocusing causes a fraction of the beam to spread away from the column, but the remaining energy of the beam resolves into a state that balances the relativistic self-focusing, defocusing, and diffraction. The power trapped in this quasistabilized state so formed is approximately 25% of the incident power.

Previous analytical estimates [38] have shown that the relativistic self-focusing length is minimal when the incident pulse intensity on the axis of the beam satisfies the condition $I_0(t)=2I_r$. Moreover, specific computations also show that this inference remains valid for the case of the relativistic self-focusing of pulses with flat initial phase fronts and Gaussian incident-transverse-intensity distributions in homogeneous plasmas.

The locus of the first focus for the case of the relativistic self-focusing has been presented previously [24]. In

that study, the beam initially had both a flat phase front and a Gaussian transverse-intensity distribution. The parameters were the same as those applying to Fig. 5(a), and the duration of the pulse corresponded to $\tau=0.5\times10^{-13}$ s. The minimal z of the locus is reached when $I_0(t)=2I_r$. If the maximum intensity on the axis of the beam is such that $I_m>2I_r$, then the trajectory of the first focus executes a path that has three reversal points. Two of them, corresponding to an identical value of z, are due to the condition $I_0(t)=2I_r$. The central one, corresponding to a greater value of z, arises when $I_0(t)=I_m$. In principle, this behavior makes it possible to distinguish the process of relativistic self-focusing from that associated with the Kerr nonlinearity, since the latter results in a locus of the first focus having only a single reversal point.

C. Relativistic and charge-displacement self-channeling

This section is devoted to the description of the self-channeling occurring when both the relativistic and charge-displacement mechanisms are included in the interaction. This situation is described by Eqs. (21)–(24) and includes the important nonlinear term involving $\nabla_\perp^2\gamma$ appearing in Eq. (24). The numerical results show that sufficiently intense short duration ($\tau_i\gg\tau\gg\tau_e$) axisymmetric pulses readily undergo self-channeling in plasmas over a rather broad range of conditions. Moreover, it is found that a large fraction of the total incident power of the beam can be trapped in a stabilized mode confined to the axis of propagation.

A specific example is informative in representing the general behavior exhibited by the propagation in the regime in which the influence of relativity and charge displacement are both significant. These results are exhibited in Fig. 6. In the case of propagation of an initially Gaussian transverse wave form incident in a homogeneous plasma, with the parameters $\lambda=0.248$ μm, $I_0=\frac{2}{3}I_r=3\times10^{19}$ W cm^{-2}, $r_0=3\mu$m, and $N_{e,0}=7.5\times10^{20}$ cm^{-3} ($a_1=248.6192$, $a_2=\frac{2}{3}$, $P_0/P_{cr}=22.252$), the numerical computations show that, as soon as the first focus on the axis of propagation is formed, electronic cavitation occurs. Specifically, this leads to *complete expulsion* of the electronic component of plasma from the paraxial domain [Fig. 6(b)]. This process results in a quasistabilized cavitated channel in the electron distribution which extends along the entire axis of propagation past the location of the initial focus [26]. We note that some of the lowest stationary solutions corresponding to the relativistic and charge-displacement problem, including cavitation, were developed by Sun *et al.* [18]. The analysis shows that the first focus involves about 45% of the total incident power of the propagating energy. A fraction of the remaining power is dissipated through diffraction on the periphery, while another component is temporarily involved in the formation of a pulsing ring-shaped structure [Fig. 6(a)]. Subsequent energy exchange between the ringlike feature and the paraxial zone is observed, and as a consequence of this interaction, a certain part of the energy of the pulsing ring is diffracted away while the remaining power joins the paraxial domain.

In finer detail, the following aspects of the evolution of the radiative energy are also revealed by the calculations. As described above, after the formation of the first focus, considerable power is transferred from the paraxial focal zone to the ring-shaped feature, which, at this stage in the evolution of the pulse, contains approximately 68% of its total initial power. This intense ring, which spreads away from the paraxial domain, produces a corresponding ring-shaped cavity in the electronic distribution [see Fig. 6(b)]. The refraction resulting from this strongly perturbed electron-density profile, together with the relativistic self-focusing mechanism, causes the wave to return energy to the core of the beam. Thus, the charge displacement produces a potent additional self-focusing action, which leads to the formation of a confined paraxial mode of high intensity stabilized along the axis of

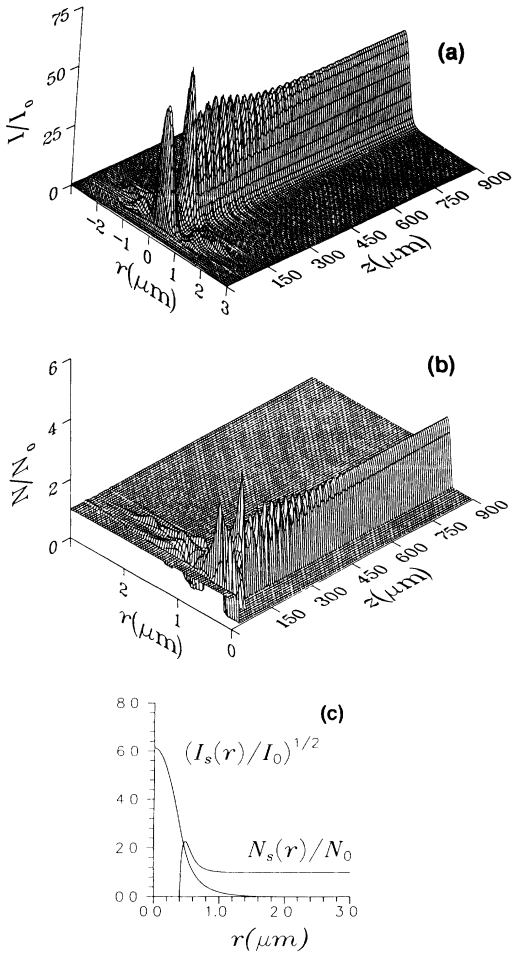

FIG. 6. The self-channeling of a pulse with a Gaussian initial transverse-intensity distribution [$N_2=2$ in Eq. (27)] and a flat incident wave front in initially homogeneous plasma in the case of the relativistic and charge-displacement propagation with $I_0=3\times10^{19}$ W/cm^2, $r_0=3$ μm, $\lambda=0.248$ μm, and $N_0=N_{e,0}=7.5\times10^{20}$ cm^{-3}. (a) The distribution of the normalized intensity. (b) The distribution of the normalized electron density. (c) Radial dependence of the asymptotic solutions for the normalized amplitude $[I_s(r)/I_0]^{1/2}$ and the normalized electron density $N_S(r)/N_0$ for $s=0.554$.

propagation. This phenomenon of confined propagation is designated as self-channeling. It should be noted that the calculations of the electrostatic energy associated with the charge displacement, which is given by the expression $W=4^{-1}\int_0^{r_c}\mathbf{E}_c^2 r\,dr$, with the electrostatic field $\mathbf{E}_c$ defined by the equation $\nabla\mathbf{E}_c=-4\pi\rho$ and r_c designating the radial extent of the channel, show that this energy can be relatively small. Specifically, for the conditions represented in Fig. 6(b) [$z=95.4$ μm], the electrostatic energy (W) accounts for only 0.18% of the total energy of the laser radiation per unit length.

The essential finding of these calculations is that the combined action of the relativistic and charge-displacement mechanisms produces a strong tendency for the generation of spatially highly confined modes of propagation which are *stabilized* along the axis of propagation. Furthermore, the study of a range of other cases indicates that these modes are exceptionally stable and that a considerable fraction of the incident power can be confined in them. The result is the controlled generation of a very high peak intensity in these channeled modes with values reaching $\sim 10^{21}$ W/cm^2 for the range of conditions studied.

Important characteristics of the asymptotic behavior of these confined modes have also been established. It has been shown that the distribution of the amplitude $u(r,z)$, for large values of z, tends asymptotically to the *lowest eigenmode* of the nonlinear Schrödinger equation (see Sec. III). Specifically, for the example discussed above, the computations have demonstrated that the asymptotic radial amplitude distribution corresponds to the lowest eigenmode with $s\simeq 0.554$. In this case, the asymptotic intensity distribution $I_s(r)=U_{s,0}^2(r)$ contains 46% of the total incident power.

The normalized asymptotic field amplitude $[I_s(r)/I_0]^{1/2}$ and the corresponding normalized asymptotic plasma electron density $N_s(r)/N_0$ are depicted in Fig. 6(c). It should be noted that the profiles of the intensity $I(r,z)$ and the electron density $N(r,z)$, obtained as the results of the dynamical calculations of the propagation for $z\simeq 900$ μm, differ from $I_s(r)$ and $N_s(r)$ for $s=0.554$ by much less than 1%. In addition, we observe that the energy of charge displacement for $r_c=2.5$ μm in the asymptotic state accounts for a fraction of 9.45×10^{-4} of the total energy of the beam per unit length. We observe that this tendency for a solution of a nonlinear Schrödinger equation involving a saturable nonlinearity to converge to the lowest stationary solution was originally discovered by Zakharov, Sobolev, and Synakh [37].

For the range of parameters studied, the calculations clearly show that the charge displacement has a very strong influence on the character of the propagation after the first focus is formed. The pulsing intensity structure, consisting of alternating foci on the axis of propagation and peripheral focal rings, which is the usual behavior for the purely relativistic self-focusing [see Figs. 5(a) and 5(b)], is converted into a stabilized and uniform channel. Collaterally, a stabilized cavitated channel in the electron density is also formed. We remark that the periodic intensity structure characteristic of the relativistic self-focusing occurs for great values of z and, therefore, may be regarded as the corresponding asymptotic solution of the purely relativistic case. The charge displacement leads to the formation of the asymptotic amplitude distribution represented by the corresponding lowest eigenmode $U_{s,0}(r)$ instead of this pulsing structure.

Computations have been also performed for the propagation of incident plateaulike wave forms with flat incident phase fronts in both homogeneous plasmas and plasma columns. Additional calculations, have also examined the behavior of focused Gaussian and plateaulike incident wave forms as well as defocused Gaussian incident wave forms in homogeneous plasmas (see Figs. 7–11). It is found that the main features described

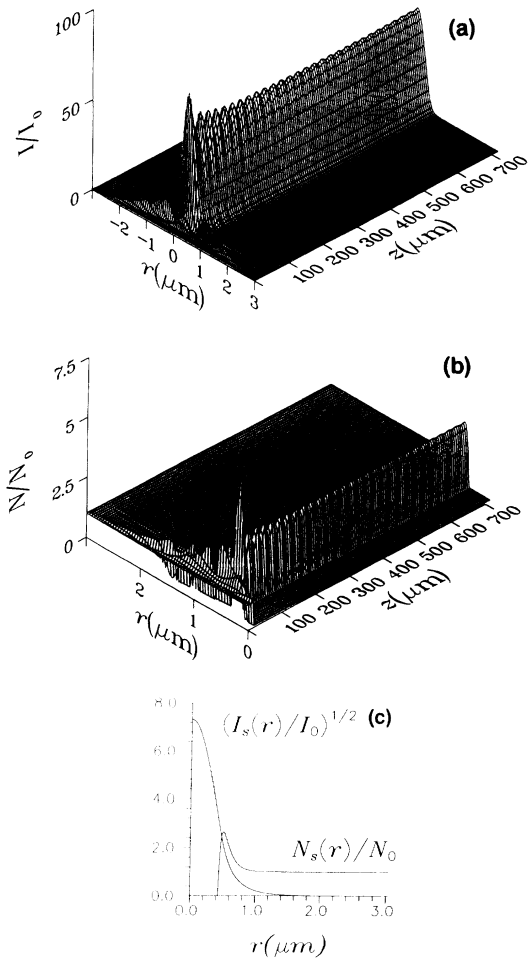

FIG. 7. The self-channeling of a pulse with a hyper-Gaussian incident-transverse-intensity distribution [$N_2=8$ in Eq. (27)] and a flat initial wave front in initially homogeneous plasma for the case of a relativistic and charge-displacement propagation with $I_0=3\times 10^{19}$ W/cm^2, $r_0=3$ μm, $\lambda=0.248$ μm, and $N_0=N_{e,0}=7.5\times 10^{20}$ cm^{-3}. (a) The distribution of the normalized intensity. (b) The distribution of the normalized electron density. (c) Radial dependence of the asymptotic solutions for the normalized amplitude $[I_s(r)/I_0]^{1/2}$ and the normalized electron density $N_s(r)/N_0$ for $s=0.515$.

above, namely (1) self-channeling, (2) stabilization of the mode of propagation, (3) the confinement of a substantial fraction of the incident power, and (4) the formation of paraxial cavitated channels in the electron distribution are common aspects of the dynamics over a wide range of conditions.

The character of these findings is now illustrated with five representative examples. For the propagation of a beam with an incident plateaulike transverse-intensity profile, given by Eq. (27) with $N_2=8$, which has a flat initial wave front incident on an initially homogeneous plasma (the values of the parameters have been adopted from above and $P_0/P_{cr}=20.168$), the asymptotic radial profile of the intensity distribution contains approximately 77% of the incident power [Fig. 7(a)]. The corresponding asymptotic amplitude is the lowest eigenmode of the nonlinear Schrödinger equation with $s\simeq 0.515$. The propagation of the same wave form in a plasma column, with the initial electron distribution defined by Eq. (29) with $N_3=8$ and $r_*=r_0$, results in a quasistabilized intensity distribution containing 34% of the incident power [Fig. 8(a)]. The purely relativistic propagation of incident plateaulike pulses [$N_2=8$ in Eq. (27)] in plasma columns [$N_3=8$ and $r_*=r_0$ in Eq. (29)] also results in the formation of quasistabilized regimes which, in this case, arise dynamically from the defocusing action of the refraction generated by the transverse profiles of the electron density [24]. For this situation, approximately 25% of the total incident power is confined [Fig. 5(d)]. The comparison of these cases with the two examples discussed above involving the charge-displacement mechanism indicates that the increase in the value of the confined power stems principally from the substantial additional focusing action arising from the inhomogeneous electron distribution produced by the ponderomotive force.

Overall, the computations reveal that the charge displacement, which generally results in electronic cavitation, plays an important role in stabilizing the mode of confined propagation that develops dynamically. This stabilization naturally occurs by refraction of the radia-

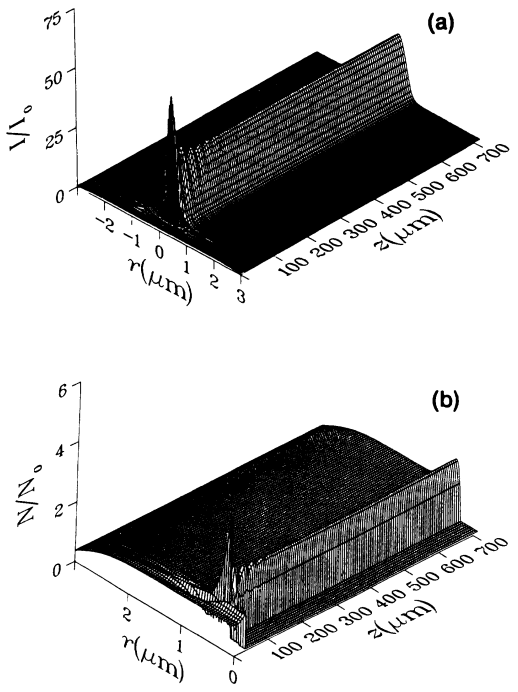

FIG. 8. The self-channeling of a pulse with a hyper-Gaussian incident-transverse-intensity distribution [$N_2=8$ in Eq. (27)] and a flat initial wave front in a preformed column-shaped plasma [$N_3=8$, $r_*=r_0$ in Eq. (29)] for the case of relativistic and charge-displacement propagation with $I_0=3\times10^{19}$ W/cm,^{2} $r_0=3$ μm, $\lambda=0.248$ μm, and $N_0=N_{e,0}=7.5\times10^{20}$ cm^{-3}. (a) The distribution of the normalized intensity. (b) The distribution of the normalized electron density.

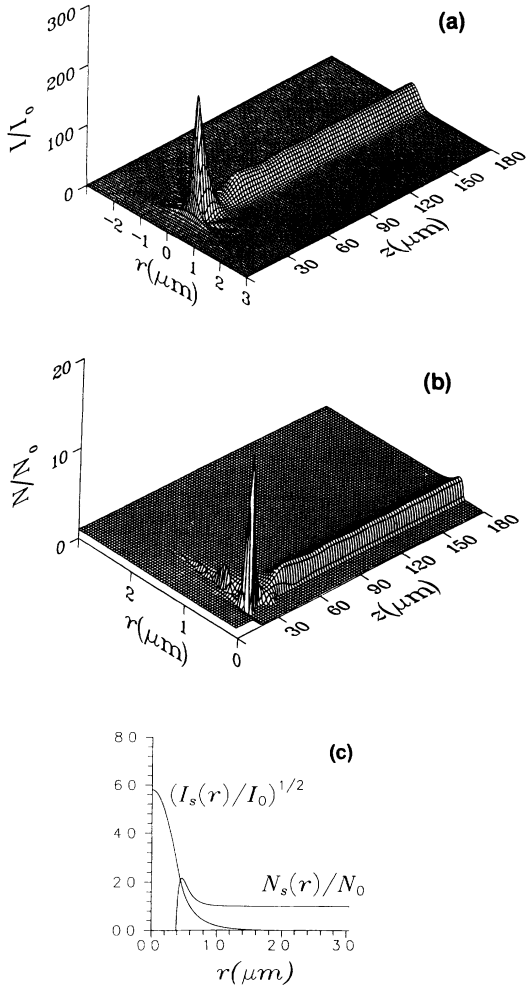

FIG. 9. Self-channeling of an initially focused [$R_f=R_{f,0}/2$ in Eq. (35)] pulse with a Gaussian incident-transverse-intensity distribution [$N_2=2$ in Eq. (35)] in initially homogeneous plasma for the case of relativistic and charge-displacement propagation with $I_0=3\times10^{19}$ W/cm^2, $r_0=3$ μm, $\lambda=0.248$ μm, and $N_0=N_{e,0}=7.5\times10^{20}$ cm^{-3}. (a) The distribution of the normalized intensity. (b) The distribution of the normalized electron density. (c) Radial dependence of the asymptotic solutions for the normalized amplitude $[I_s(r)/I_0]^{1/2}$ and the normalized electron density $N_s(r)/N_0$ for $s=0.566$.

tion into the central paraxial region. Indeed, the influence of the charge displacement on the propagation is so strong that self-channeling occurs even in the cases of *extremely* focused and defocused incident wave forms. The results of the corresponding calculations for extremely focused incident wave forms, for $R_f = R_{f,0}/2$ [Eq. (35)], with both Gaussian [$N_2 = 2$ in Eq. (35)] and plateaulike [$N_2 = 8$ in Eq. (35)] incident-transverse-intensity distributions, are depicted in Figs. 9 and 10, respectively (the parameters of beam and plasma being the same as the other examples above). In these two cases, the asymptotic transverse profiles of the amplitude and the electron density are found to correspond to the lowest eigenmodes of the nonlinear Schrödinger equation with values of the parameter $s \simeq 0.566$ (Fig. 9) and $s \simeq 0.505$ (Fig. 10). Note, in strong contrast to the situation involving charge displacement, the analogously strongly focused incident wave forms for the purely relativistic case propagate in the single-focus regime [Fig. 5(c)], and stable confinement does not develop.

Figure 11 illustrates the relativistic and charge-displacement propagation of an initially strongly defocused wave form [$R_f = -R_{f,0}/2$ in Eq. (35)] having a Gaussian initial transverse-intensity distribution [$N_2 = 2$ in Eq. (35)]. After the initial stage of the defocusing, this pulse evolves into a paraxial structure that is analogous to those described above. Furthermore, in this example the asymptotic transverse profiles of the amplitude and the electron density are found to correspond to the lowest eigenmode of the nonlinear Schrödinger equation with

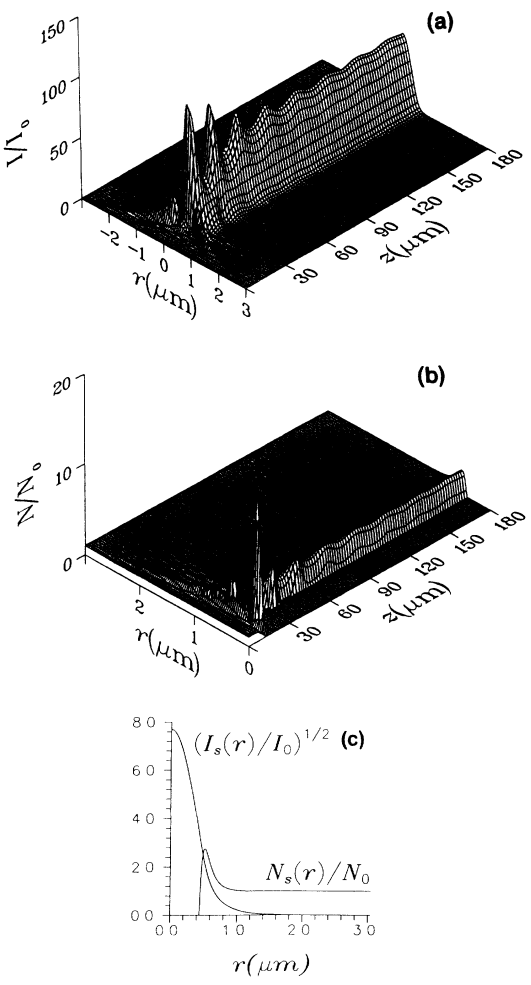

FIG. 10. The self-channeling of an initially focused [$R_f = R_{f,0}/2$ in Eq. (35)] pulse with a hyper-Gaussian incident-transverse-intensity distribution [$N_2 = 8$ in Eq. (35)] in initially homogeneous plasma for the case of relativistic and charge-displacement propagation with $I_0 = 3 \times 10^{19}$ W/cm^2, $r_0 = 3$ μm, $\lambda = 0.248$ μm, and $N_0 = N_{e,0} = 7.5 \times 10^{20}$ cm^{-3}. (a) The distribution of the normalized intensity. (b) The distribution of the normalized electron density. (c) Radial dependence of the asymptotic solutions for the normalized amplitude $[I_s(r)/I_0]^{1/2}$ and the normalized electron density $N_s(r)/N_0$ for $s = 0.505$.

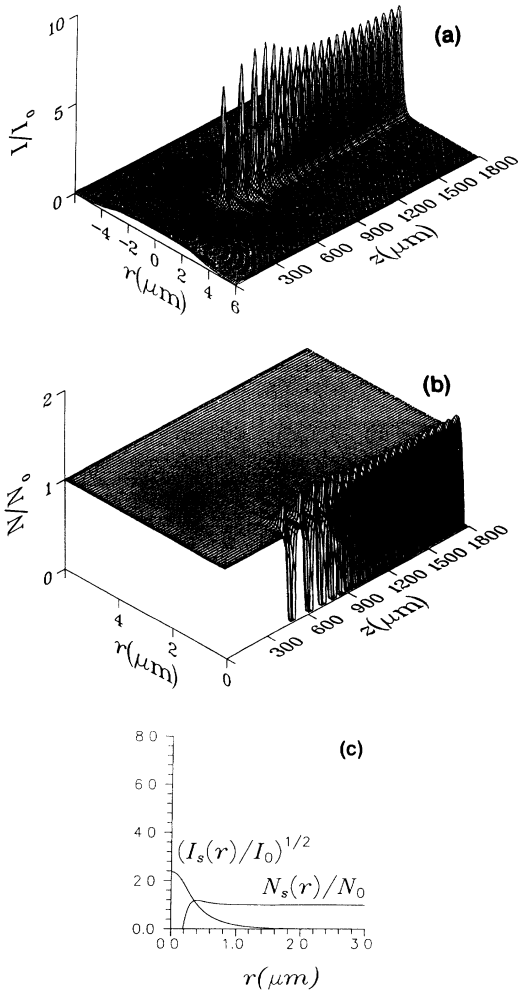

FIG. 11. The self-channeling of an initially defocused [$R_f = -R_{f,0}/2$ in Eq. (35)] pulse with a Gaussian incident-transverse-intensity distribution [$N_2 = 2$ in Eq. (35)] in initially homogeneous plasma for the case of relativistic and charge-displacement propagation with $I_0 = 3 \times 10^{19}$ W/cm^2, $r_0 = 3$ μm, $\lambda = 0.248$ μm, and $N_0 = N_{e,0} = 7.5 \times 10^{20}$ cm^{-3}. (a) The distribution of the normalized intensity. (b) The distribution of the normalized electron density. (c) Radial dependence of the asymptotic solutions for the normalized amplitude $[I_s(r)/I_0]^{1/2}$ and the normalized electron density $N_s(r)/N_0$ for $s = 0.800$.

$s \simeq 0.800$.

For these values of the dimensionless parameters assumed in these examples (Figs. 9–11) ($a_1 = 248.6192$, $a_2 = \frac{2}{3}$, that is $P_0/P_{cr} = 22.252$ for Gaussian incident wave form), the magnitude of the quantity $R_f = R_{f,0}/2$, the factor determining the degree of the initial focusing (defocusing), is 0.124. For $\lambda = 0.248$ μm and $r_0 = 3$ μm, the focusing distance $R = kr_0^2 R_{f,0}/2$, used in the examples above, has a magnitude of 28.35 μm. The fact that the self-channeling of such extremely focused or defocused distributions occurs (Figs. 9–11) means the self-channeling should be expected to be nearly independent of the initial conditions of focusing or defocusing.

A critical power P_{cr} for self-channeling arising from the relativistic charge-displacement mechanism can be defined. We now discuss this issue with a model developed in an earlier study. The threshold power P_{cr} is defined as the power that separates the asymptotic behavior, with respect to large distance of propagation (z), into two distinct classes. Since its definition rests on an asymptotic property, it can only exist in the limiting case of vanishing losses ($\mu = 0$ in Ref. [24]). For a power $P < P_{cr}$, the asymptotic transverse-intensity profile tends to zero at large z. In contrast, for $P \geq P_{cr}$ the asymptotic profile of the intensity tends to the lowest eigenmode of the governing nonlinear Schrödinger equation. Additionally, the normalized value of this critical power is exactly *twice* the corresponding normalized value of the critical power for the Kerr effect self-focusing found in cubic media for initially flat wave forms [34,37]. The expression corresponding to this critical power [36] for the relativistic and charge-displacement mechanism is

$$P_{cr} = (m_{e,0}^2 c^5/e^2) \int_0^\infty g_0^2(\rho) \rho \, d\rho (\omega/\omega_{p,0})^2 \simeq 1.6198 \times 10^{10} (\omega/\omega_{p,0})^2 \text{ W} , \tag{36}$$

where $g_0(\rho)$ is the Townes mode [34].

It has also been shown that the value of the relativistic and charge-displacement self-channeling threshold power, in cases involving initially focused or defocused beams, exceeds P_{cr} and depends on the degree of the initial focusing or defocusing. For a given magnitude of the curvature of the wave front, the value of the threshold power for initially defocused beams is greater than that for initially focused beams. Finally, it has been shown both analytically and numerically that for self-channeling of an arbitrary wave form to occur, it is sufficient that the Hamiltonian of the purely relativistic case, considered as a functional of the initial transverse amplitude distribution, should be negative [36]. The precise statement for this condition is

$$P_2(u_0) = \int_0^\infty \left[\left| \frac{du_0}{dr} \right|^2 - a_1 \{ |u_0|^2 - (2/a_2)[(1+a_2|u_0|^2)^{1/2} - 1] \} \right] r \, dr < 0 . \tag{37}$$

We now comment on the behavior of pulses having initial amplitude distributions $U_0(r)$ close to higher eigenmodes $V_{s,n}(r)$, $n \geq 1$. These higher modes generally are associated with electronically cavitated channels. The self-channeling in these cases could result in asymptotic distributions of intensity and electron density corresponding to certain higher eigenfunctions $I_{s,n}(r) = V_{s,n}^2(r)$, $N_{s,n}(r)$, $n \geq 1$. In particular, this conjecture has established an initial amplitude distribution $U_0(r)$, which is close to the first eigenmode $V_{s,1}(r)$ with $s = 0.544$. Direct numerical calculations showed that the asymptotic distributions of both intensity and electron density that evolved in this case correspond to the first eigenmode $I_{s,r}(r) = V_{s,r}^2(r)$, $N_{s,1}(r)$ with s essentially equal to 0.544. It should be additionally noted, however, that these higher eigenmodes ($n \geq 1$) are quite possibly unstable against small azimuthal perturbations that destroy their axial symmetry.

The principal result of this section is the finding that the combined action of the relativistic and charge-displacement mechanisms can result in self-channeling with the formation of stabilized paraxial modes over a rather wide range of physical conditions. Moreover, these spatially confined modes are generally associated with corresponding cavitated channels in the electron density. Finally, the characteristics of these channeled modes have asymptotic behavior that is described by the appropriate lowest eigenmodes of the governing nonlinear Schrödinger equation.

V. CONCLUSIONS

A theoretical approach suitable for the numerical investigation of the two-dimensional (r,z) dynamics of propagation of coherent ultrashort ($\tau_i \gg \tau \gg \tau_e$) relativistic laser pulses in cold underdense plasmas has been developed. Four basic physical phenomena are included within the scope of this method. They are (1) the nonlinear dependence of the index of refraction due to the relativistic increase in the mass of the electrons, (2) the variation of the index of refraction resulting from the perturbation of the electron density by the ponderomotive force, (3) the diffraction of the radiation, and (4) the refraction caused by nascent transversely inhomogeneous electron-density distributions. The equations studied in this work may be regarded as the generalization of those treated previously in other studies [18,19,33] involving initially inhomogeneous plasmas. Further studies are continuing with an extension of this analysis, which includes the azimuthal coordinate in the description of the propagation.

The main conclusions stemming from the calculations are the following.

(1) The cooperative effect of the relativistic and charge-displacement mechanisms leads asymptotically to stable high-intensity z-independent modes of self-channeling, and a major fraction of the incident power can be confined in these paraxial modes. Stable cavitation of the electron density is a general feature of these spatially confined modes.

(2) The z-independent modes, to which the solutions of the equation describing the relativistic and charge-displacement propagation tend asymptotically, are recognized as the *lowest* eigenmodes of the governing nonlinear Schrödinger equation.

(3) A separate study of purely relativistic propagation shows that beams with flat incident phase fronts exhibit a pulsing behavior in homogeneous plasmas but can undergo quasistabilization in suitably configured plasma columns. However, sufficiently sharply initially focused beams generally exhibit the development of only a single focus. In significant contrast, the present study shows that with both the relativistic and charge-displacement mechanisms, initially focused beams also generally lead to confined modes of propagation. Finally, it should be noted that the equation for relativistic self-focusing can be considered as a general model equation of propagation in saturable nonlinear media.

ACKNOWLEDGMENTS

The authors acknowledge fruitful discussions with A. R. Hinds, R. R. Goldstein, and A. McPherson. Support for this research was provided by the U.S. Air Office of Scientific Research, the U.S. Office of Naval Research, the Strategic Defense Initiative Organization, the Army Research Office, the Department of Energy, and the National Science Foundation under Grant No. PHY-9021265.

*Present address: Department of Physics, University of Illinois at Chicago, Chicago, Illinois 60680.

[1] U. Johann, T. Luk, H. Egger, and C. K. Rhodes, Phys. Rev. A **34**, 1084 (1986).

[2] T. S. Luk, U. Johann, H. Egger, H. Pummer, and C. K. Rhodes, Phys. Rev. A **32**, 214 (1985); K. Boyer, T. S. Luk, J. C. Solem, and C. K. Rhodes, *ibid.* **39**, 1186 (1989).

[3] A. I. Akhiezer and R. V. Polovin, Zh. Eksp. Teor. Fiz. **30**, 915 (1956) [Sov. Phys. JETP **3**, 696 (1956)].

[4] R. Noble, Phys. Rev. A **32**, 460 (1985).

[5] A. Magneville, J. Plasma Phys. **44**, 231 (1990).

[6] S. V. Bulanov, V. I. Kirsanov, and A. S. Sakharov, Fiz. Plasmy **16**, 935 (1990) [Sov. J. Plasma Phys. **16**, 543 (1990)].

[7] P. Sprangle, E. Esarey, and A. Ting, Phys. Rev. Lett. **64**, 2011 (1990); P. Sprangle, C. M. Tang, and E. Esarey, Phys. Rev. A **41**, 4663 (1990); A. Ting, E. Esarey, and P. Sprangle, Phys. Fluids **B2**, 1390 (1990).

[8] L. D. Landau and E. M. Lifshits, *The Classical Theory of Fields* (Pergamon, New York, 1971).

[9] E. S. Sarachik and G. T. Schappert, Phys. Rev. D **1**, 2738 (1970).

[10] J. Krüger and M. Bovyn, J. Phys. A **9**, 1841 (1976).

[11] D. M. Volkov, Z. Phys. **34**, 250 (1935).

[12] J. N. Bardsley, B. M. Penetrante, and M. H. Mittleman, Phys. Rev. A **40**, 3823 (1989).

[13] C. Max, J. Arons, and A. B. Langon, Phys. Rev. Lett. **33**, 209 (1974).

[14] G. Schmidt and W. Horton, Comments Plasma Phys. Controlled Fusion **9**, 85 (1985).

[15] H. Hora, *Physics of Laser-Driven Plasmas* (Wiley, New York, 1981).

[16] P. Sprangle and C. M. Tang, in *Laser Acceleration of Particles (the Norton Simon Malibu Beach Conference Center of the University of California, Los Angeles)*, Proceedings of the Second Workshop on Laser Acceleration of Particles, edited by C. Joshi and T. Katsouleas, AIP Conf. Proc. No. 130 (AIP, New York, 1985), p. 156.

[17] P. Sprangle, C. M. Tang, and E. Esarey, IEEE Trans. Plasma **PS-15**, 145 (1987).

[18] Gou-Zheng Sun, E. Ott, Y. C. Lee, and P. Guzdar, Phys. Fluids **30**, 526 (1987).

[19] T. Kurki-Suonio, P. J. Morrison, and T. Tajima, Phys. Rev. A **40**, 3230 (1989).

[20] E. Esarey, A. Ting, and P. Sprangle, Appl. Phys. Lett. **53**, 1266 (1988).

[21] W. B. Mori, C. Joshi, J. M. Dawson, D. W. Forslund, and J. M. Kindel, Phys. Rev. Lett. **60**, 1298 (1988).

[22] P. Gibbon and A. R. Bell, Phys. Rev. Lett. **61**, 1599 (1988).

[23] C. J. McKinstrie and D. A. Russel, Phys. Rev. Lett. **61**, 2929 (1988).

[24] A. B. Borisov, A. V. Borovskiy, V.V. Korobkin, A. M. Prokhorov, C. K. Rhodes, and O. B. Shiryaev, Phys. Rev. Lett. **65**, 1753 (1990).

[25] J. C. Solem, T. S. Luk, K. Boyer, and C. K. Rhodes, IEEE J. Quantum Electron. **25**, 2423 (1989).

[26] A. B. Borisov, A. V. Borovskiy, V. V. Korobkin, A. M. Prokhorov, O. B. Shiryaev, T. S. Luk, J. C. Solem, K. Boyer, and C. K. Rhodes (unpublished); A. B. Borisov, A. V. Borovskiy, V. V. Korobkin, A. M. Prokhorov, O. B. Shiryaev, J. C. Solem, K. Boyer, and C. K. Rhodes (unpublished); A. B. Borisov, A. V. Borovskiy, V. V. Korobkin, A. M. Prokhorov, O. B. Shiryaev, and C. K. Rhodes, Kratkie Soobsheniya po Fizike, No. 9, 3 (1991) (in Russian).

[27] A. B. Borisov, A. V. Borovskiy, V. V. Korobkin, A. M. Prokhorov, O. B. Shiryaev, X. M. Shi, T. S. Luk, A. McPherson, J. C. Solem, K. Boyer, and C. K. Rhodes (unpublished).

[28] T. S. Luk and C. K. Rhodes, Phys. Rev. A **38**, 6180 (1988).

[29] G. A. Askaryan, Zh. Eksp. Teor. Fiz. **42**, 1567 (1962) [Sov. Phys. JETP **15**, 1088 (1962)].

[30] T. S. Luk, A. McPherson, K. Boyer, and C. K. Rhodes, Opt. Lett. **14**, 1113 (1989).

[31] A. J. Taylor, C. R. Tallman, J. P. Roberts, C. S. Lester, T. R. Gosnell, P. H. Y. Lee, and G. A. Kyrala, Opt. Lett. **15**, 39 (1990).

[32] P. Maine, D. Strickland, P. Bado, M. Pessot, and G. Mourou, IEEE J. Quantum Electron. **24**, 398 (1988).

[33] P. Sprangle, A. Zigler, and E. Esarey, Appl. Phys. Lett. **58**, 345 (1991).

[34] R. Y. Chiao, E. Garmire, and C. H. Townes, Phys. Rev. Lett. **13**, 479 (1964).

[35] H. A. Haus, Appl. Phys. Lett. **8**, 128 (1966).

[36] A. B. Borisov, A. V. Borovskiy, V. V. Korobkin, A. M. Prokhorov, O. B. Shiryaev, and C. K. Rhodes, J. Laser Phys. **1**, 103 (1991).

[37] V. E. Zakharov, V. V. Sobolev, and V. S. Synakh, Zh. Eksp. Teor. Fiz. **60**, 136 (1971) [Sov. Phys. JETP **33**, 77 (1971)].

[38] A. B. Borisov, A. V. Borovskiy, V. V. Korobkin, C. K. Rhodes, and O. B. Shiryaev (unpublished); A. B. Borisov, A. V. Borovskiy, V. V. Korobkin, C. K. Rhodes, and O. B. Shiryaev, in *Short Wavelength Lasers and Their Applications,* edited by V. V. Korobkin and M. Yu. Romanovskiy (Nova Science, Commack, NY, 1992), p. 261.

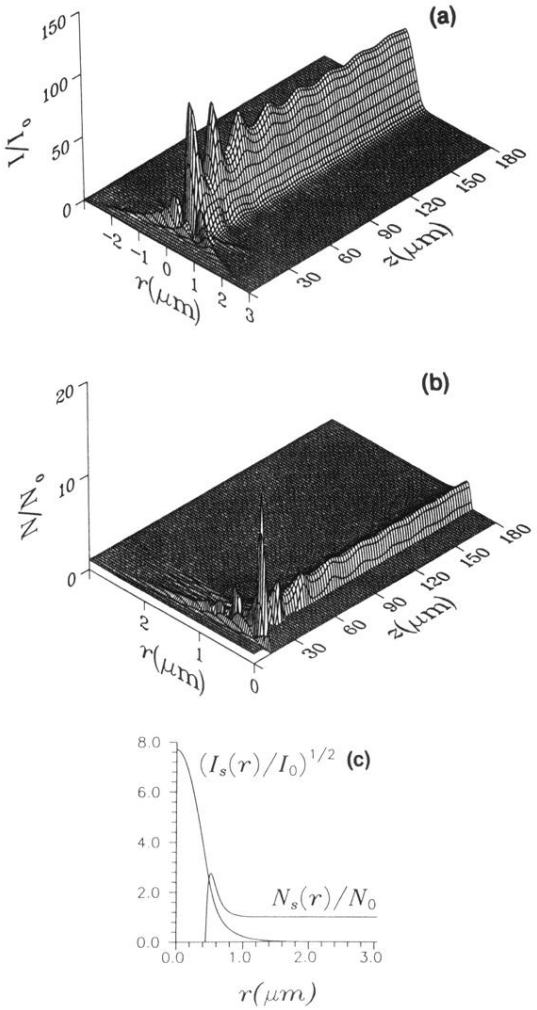

FIG. 10. The self-channeling of an initially focused [$R_f = R_{f,0}/2$ in Eq. (35)] pulse with a hyper-Gaussian incident-transverse-intensity distribution [$N_2 = 8$ in Eq. (35)] in initially homogeneous plasma for the case of relativistic and charge-displacement propagation with $I_0 = 3 \times 10^{19}$ W/cm^2, $r_0 = 3$ μm, $\lambda = 0.248$ μm, and $N_0 = N_{e,0} = 7.5 \times 10^{20}$ cm^{-3}. (a) The distribution of the normalized intensity. (b) The distribution of the normalized electron density. (c) Radial dependence of the asymptotic solutions for the normalized amplitude $[I_s(r)/I_0]^{1/2}$ and the normalized electron density $N_s(r)/N_0$ for $s = 0.505$.

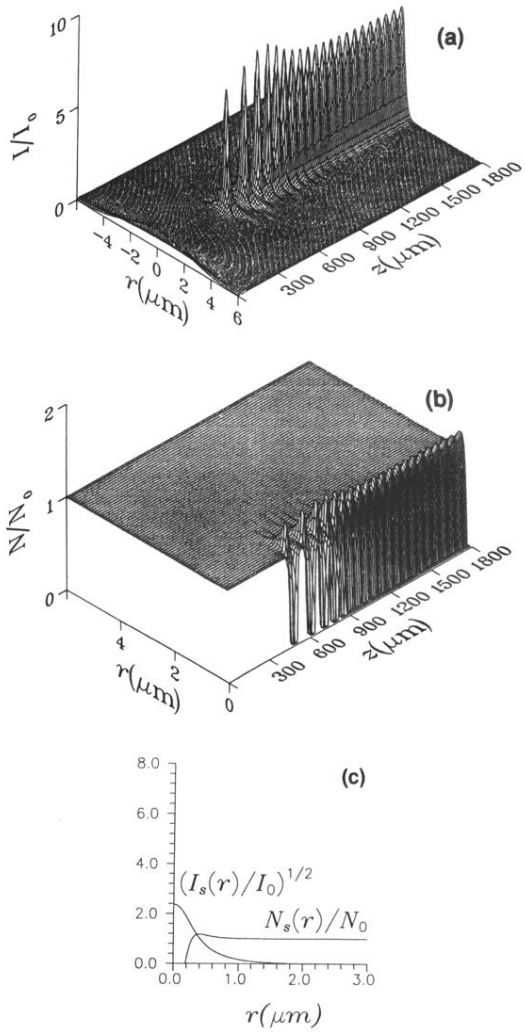

FIG. 11. The self-channeling of an initially defocused [$R_f = -R_{f,0}/2$ in Eq. (35)] pulse with a Gaussian incident-transverse-intensity distribution [$N_2 = 2$ in Eq. (35)] in initially homogeneous plasma for the case of relativistic and charge-displacement propagation with $I_0 = 3 \times 10^{19}$ W/cm^2, $r_0 = 3$ μm, $\lambda = 0.248$ μm, and $N_0 = N_{e,0} = 7.5 \times 10^{20}$ cm^{-3}. (a) The distribution of the normalized intensity. (b) The distribution of the normalized electron density. (c) Radial dependence of the asymptotic solutions for the normalized amplitude $[I_s(r)/I_0]^{1/2}$ and the normalized electron density $N_s(r)/N_0$ for $s = 0.800$.

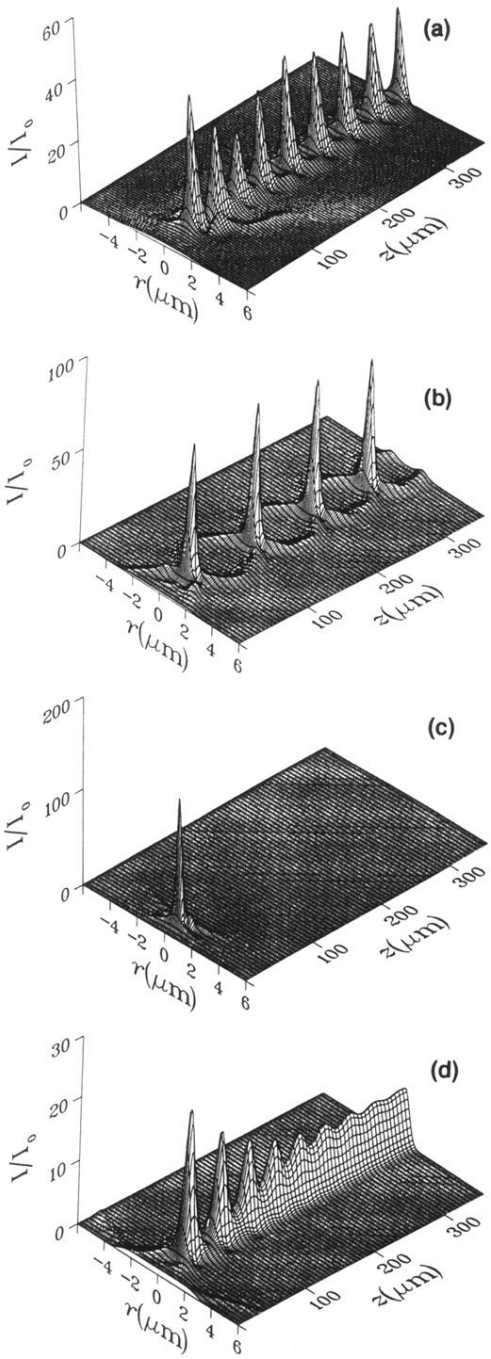

FIG. 5. Purely relativistic propagation with $I_0=3\times10^{19}$ W/cm^2, $r_0=3$ μm, $\lambda=0.248$ μm, and $N_{e,0}=7.5\times10^{20}$ cm^{-3}. (a) The formation of the pulsing waveguide regime in the case of the relativistic self-focusing of a pulse with a flat incident wave front; Gaussian initial transverse-intensity distribution [$N_2=2$ in Eq. (27)], homogeneous plasma. (b) The formation of the pulsing waveguide regime in the case of the relativistic self-focusing of a pulse with a flat incident wave front; hyper-Gaussian initial transverse-intensity distribution [$N_2=8$ in Eq. (27)], homogeneous plasma. (c) The single-focus regime in the case of the relativistic self-focusing of an initially focused pulse [$R_f=R_{f,0}/2$ in Eq. (35)]; Gaussian incident-transverse-intensity distribution [$N_2=2$ in Eq. (35)], homogeneous plasma. (d) The formation of the quasistabilized regime in the case of the relativistic self-focusing of a pulse with a flat incident wave front in a plasma column [$N_3=8$, $r_*=r_0$ in Eq. (29)]; hyper-Gaussian initial transverse-intense distribution [$N_2=8$ in Eq. (27)].

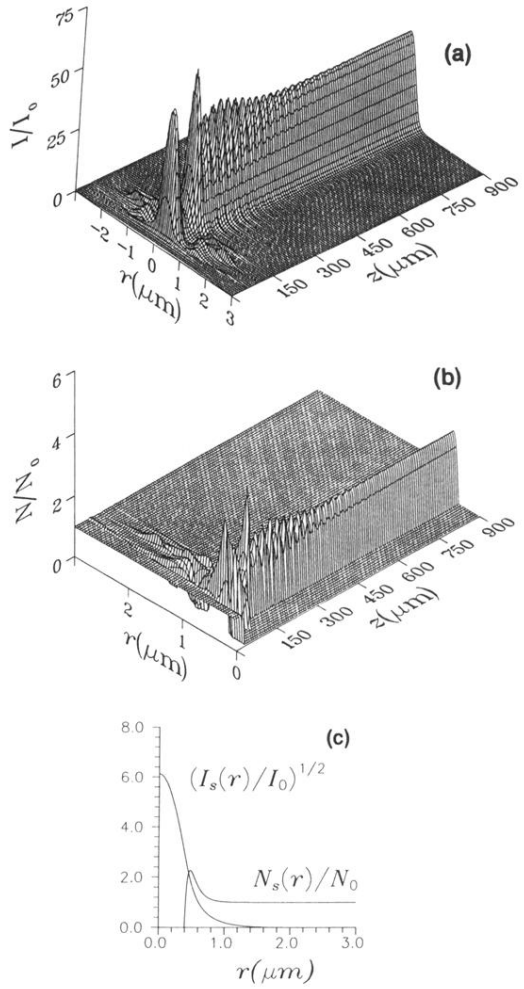

FIG. 6. The self-channeling of a pulse with a Gaussian initial transverse-intensity distribution [$N_2=2$ in Eq. (27)] and a flat incident wave front in initially homogeneous plasma in the case of the relativistic and charge-displacement propagation with $I_0=3\times10^{19}$ W/cm^2, $r_0=3$ μm, $\lambda=0.248$ μm, and $N_0=N_{e,0}=7.5\times10^{20}$ cm^{-3}. (a) The distribution of the normalized intensity. (b) The distribution of the normalized electron density. (c) Radial dependence of the asymptotic solutions for the normalized amplitude $[I_s(r)/I_0]^{1/2}$ and the normalized electron density $N_S(r)/N_0$ for $s=0.554$.

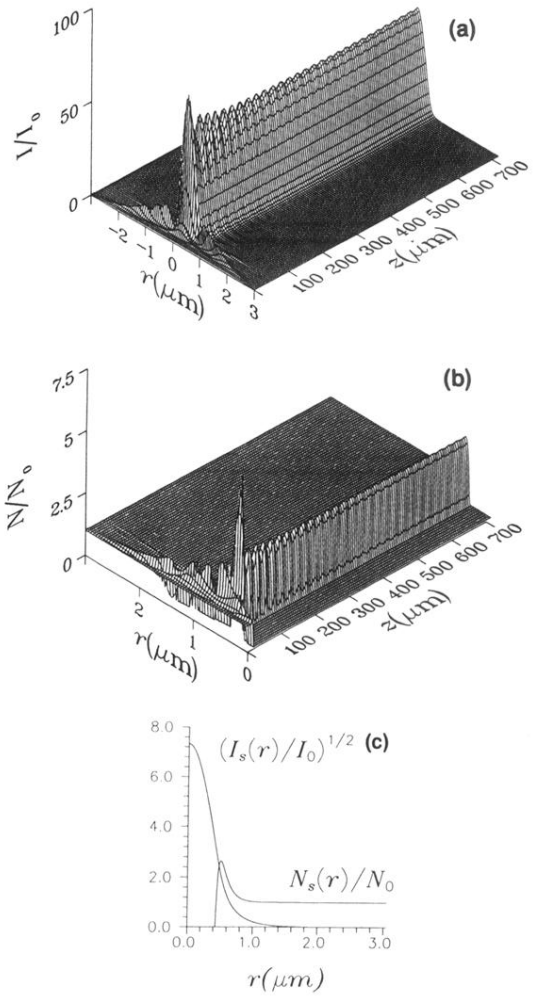

FIG. 7. The self-channeling of a pulse with a hyper-Gaussian incident-transverse-intensity distribution [$N_2=8$ in Eq. (27)] and a flat initial wave front in initially homogeneous plasma for the case of a relativistic and charge-displacement propagation with $I_0=3\times10^{19}$ W/cm^2, $r_0=3$ μm, $\lambda=0.248$ μm, and $N_0=N_{e,0}=7.5\times10^{20}$ cm^{-3}. (a) The distribution of the normalized intensity. (b) The distribution of the normalized electron density. (c) Radial dependence of the asymptotic solutions for the normalized amplitude $[I_s(r)/I_0]^{1/2}$ and the normalized electron density $N_s(r)/N_0$ for $s=0.515$.

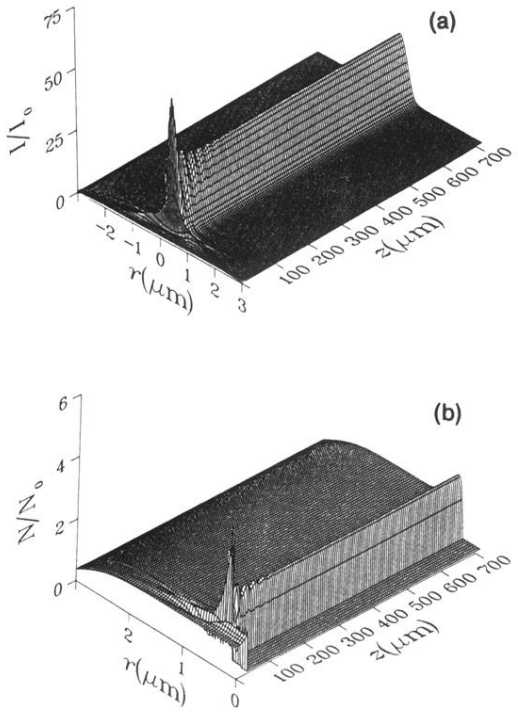

FIG. 8. The self-channeling of a pulse with a hyper-Gaussian incident-transverse-intensity distribution [$N_2=8$ in Eq. (27)] and a flat initial wave front in a preformed column-shaped plasma [$N_3=8$, $r_*=r_0$ in Eq. (29)] for the case of relativistic and charge-displacement propagation with $I_0=3\times10^{19}$ W/cm,^{2} $r_0=3$ μm, $\lambda=0.248$ μm, and $N_0=N_{e,0}=7.5\times10^{20}$ cm^{-3}. (a) The distribution of the normalized intensity. (b) The distribution of the normalized electron density.

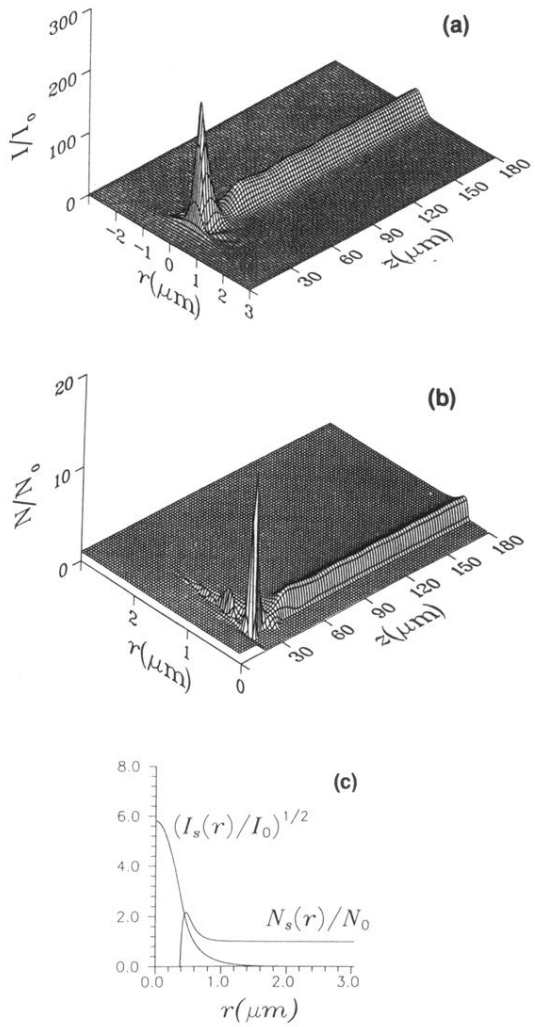

FIG. 9. Self-channeling of an initially focused [$R_f = R_{f,0}/2$ in Eq. (35)] pulse with a Gaussian incident-transverse-intensity distribution [$N_2 = 2$ in Eq. (35)] in initially homogeneous plasma for the case of relativistic and charge-displacement propagation with $I_0 = 3 \times 10^{19}$ W/cm^2, $r_0 = 3$ μm, $\lambda = 0.248$ μm, and $N_0 = N_{e,0} = 7.5 \times 10^{20}$ cm^{-3}. (a) The distribution of the normalized intensity. (b) The distribution of the normalized electron density. (c) Radial dependence of the asymptotic solutions for the normalized amplitude $[I_s(r)/I_0]^{1/2}$ and the normalized electron density $N_s(r)/N_0$ for $s = 0.566$.